Journal of Polymer Research (2020) 27: 140
https://doi.org/10.1007/s10965-020-02090-9

REVIEW PAPER

Influence of chemical structure of hard segments on physical properties of polyurethane elastomers: a review

Ken Kojio[1,2,3] · Shuhei Nozaki[2] · Atsushi Takahara[1,2,3] · Satoshi Yamasaki[4]

Received: 25 October 2019 / Accepted: 25 March 2020 / Published online: 7 May 2020

Abstract

Hard segments of polyurethanes (PUs) are generally formed from diisocyanate and diol. Diol can be replaced with triol and thiol. These chemical structures of hard segments strongly affect not only a microphase separated structure but mechanical properties of resultant PUs. In this review, we focus on the relationship between chemical structure like symmetry and bulkiness of diisocyanate and mechanical properties of PU. Then, influence of hard segment content, incorporation of 1,1,1-trimethylol propane with trifunctional groups, and alkyldithiol was reviewed mainly on *trans*-1,4-bis(isocyanatomethyl) cyclohexane-poly(oxytetramethylene) glycol-based PU.

Keywords Polyurethane · Diisocyanate · Polymer glycol · Hard segment · Microphase-separated structure · Mechanical property

Introduction

Elastomeric materials have important roles for our life, for instance, tires, elastic fibers, hoses, and so on. Without tires, we cannot use both airplanes and vehicles. There are many types of elastomers such as natural rubber, styrenic triblock copolymers, polyurethane (PU), and polyamide elastomers. PU is one of the representative elastomers which can be applied for various applications due to an ease to tune various mechanical properties [1–6]. For instance, Young's modulus and elongation at break can be varied from MPa to GPa and from 0.1 to 10, respectively. In case of segmented s, they generally consist of flexible soft segment and rigid hard segment. There are many types of rubbery chains, which is an indispensable component to exhibit elastic property of polymers, ether polymer glycols [5–11], ester polymer glycols [5, 6, 12–14], carbonate polymer glycols [15–23], and aliphatic polymer glycols [5, 6, 24]. To optimize demanded properties, appropriate polyol needs to be chosen in terms of mechanical property, resistances for hydrolysis and environment, temperature characteristics, and so on. Another component is a hard segment, which works as cross-linking points to connect rubbery chains together. The hard segment is comprised of isocyanate and chain extender. There are tremendous numbers of diisocyanate and chain extender, such as aromatic [5, 6, 25, 26], aliphatic [10, 27–29] and cycloaliphatic ones [10, 13, 30–40]. A chemical structure of these ingredients strongly affects the states of hydrogen bonding and crystallization of hard segments. Needless to say, these states are closely related to not only a microphase-separated structure but various properties of PUs. Thus, it is quite important to control them. Relationship between types of soft and hard segments and various properties of elastomer in literature will be described in the later section in detail.

Application of PU to elastomer is one of the most popular ways. Another application of PU is coating, adhesive, sealant, fibers, and so on. Many researchers are still working on to improve and create new property. Non-isocyanate-based PUs [41–47], (PU/crystalline polymer) blends [48], (PU/inorganic filler) composites [49, 50], PUs with dynamic covalent bonds [51, 52], self-healing PU [53, 54], PU incorporating rotaxane [55, 56], waterborne PU [57–63], thin and ultrathin PU films [11, 64–67], comb-shaped PU [68], can be given as examples. Concerning about non-isocyanate-based PUs,

✉ Ken Kojio
kojio@cstf.kyushu-u.ac.jp

[1] Institute for Materials Chemistry and Engineering, Kyushu University, 744 Motooka, Nishi-ku, Fukuoka 819-0395, Japan

[2] Graduate School of Engineering, Kyushu University, 744 Motooka, Nishi-ku, Fukuoka 819-0395, Japan

[3] WPI-I2CNER, Kyushu University, 744 Motooka, Nishi-ku, Fukuoka 819-0395, Japan

[4] Mitsui Chemicals, Inc., 580-32, Nagaura, Sodegaura, Chiba 299-0265, Japan

Endo et al. reported synthesis of poly(hydroxyurethane)s from five-membered cyclic carbonate and diamine and their various properties [41–43]. Torkelson et al. investigated that molecular aggregation structure and mechanical properties of segmented poly(hydroxyurethane)s synthesized with various bis-carbonate molecules, diamine and polyether glycol [44–46]. In many cases of applications, mechanical strength, like tensile strength and scratch resistance of PUs, is always the point, which should be considered.

There are some factors to control mechanical properties of PU. (1) The degree of microphase separation, (2) aggregation force of hard segment chains (hydrogen bond and crystallization), (3) density of physical and chemical cross-linking network, (4) inhomogeneity of the network, (5) ability of orientation and crystallization of soft segment, (6) entanglement density, and (7) ability of hopping of hard segment during deformation can be given as examples. These states mentioned above have been investigated by Fourier-transform infrared spectroscopy (FT-IR) [69–72], small-angle X-ray scattering (SAXS) [19, 33–36, 38, 73–80], wide-angle X-ray diffraction (WAXD) [81–85], and atomic force microscopy (AFM) [11, 67, 86–89], and so on. As the results, combination of MDI, BD, and PTMO can be given as one of the representative PU with high mechanical properties [90, 91]. This is because MDI and BD-based hard segment domains can crystallize with the formation of hydrogen bonds [5, 82, 85].

In this review, the effect of chemical structure of diisocyanate on physical properties of elastomer will be introduced in the first part. Isophorone diisocyanate (IPDI), norbornene diisocyanate (NBDI), 1,3-phenylene diisocyanate (MPDI), *trans*-1,3-bis(isocyanatomethyl) cyclohexane (1,3-H_6XDI), bicyclohexylmethane-4,4′-diisocyanate (HMDI), 4,4′-diphenylmethane diisocyanate (MDI), *trans*-1,3-bis(isocyanatomethyl) cyclohexane (1,4-H_6XDI), 1,4-cyclohexyl diisocyanate (CHDI), and 1,4-phenylene diisocyanate (PPDI) were used as diisocyanate for synthesis of PU. In the second, third and fourth parts, effects of hard segment content, chemical cross-linking points, and chain extender of thiols on the PU were briefly introduced from literature in each section and discussed using our results of 1,4-H_6XDI-PTMG-based PUs. In the final part, mechanical deformation behavior was summarized using our results of 1,4-H_6XDI-PTMG-thiol-based PU as an example.

Chemical structure of diisocyanate

Figure 1 shows chemical structure of aromatic, aliphatic and cycloaliphatic diisocyanates shown in this review. Symmetry, steric hindrance, and periodic distance between isocyanate groups affect not only the aggregation structure of hard segment chains but the microphase-separated structure.

Hepburn et al. [13] used HMDI, TDI, MDI, PPDI and CHDI as diisocyanate and polycaprolactone as polyol and conducted temperature dependence of dynamic viscoelastic properties measurement. The magnitude of dynamic storage modulus (*E'*) at the rubbery plateau region was following order: CHDI > PPDI > MDI > TDI > HMDI. Furthermore, terminal flow of CHDI-based PU showed 20 °C higher than for others. It is inferred that these trends can be ascribed to the degree of microphase separation of CHDI-based PU is higher than others. Yilgor et al. reported direct evidence for PPDI- and MPDI-based PU with PTMG using dynamic viscoelastic measurement [38, 92, 93] and atomic force microscopy and PPDI-, CHDI-, MDI-, and HMDI-based PU with PTMG by infrared spectroscopy [37, 38]. The relationship between symmetry of chemical structure of diisocyanate and mechanical properties is strongly related each other. Kinked, and asymmetric diisocyanate exhibited higher glass transition temperature of PTMG chain, the lower *E'* value at the rubbery plateau region and lower heat resistance, which were confirmed by low hydrogen bonds phase separation by infrared spectroscopy. In contrast, symmetric diisocyanate showed self-organization and formation of well-ordered hard segments, resulting in higher magnitude of *E'* at the rubbery plateau region and higher heat resistance.

On the other hand, the authors have investigated thermal behavior of the hard segment chains of four types of diisocyanates including aliphatic and cycloaliphatic ones. Hard segment models were synthesized from diisocyanates and BD [10]. Figure 2 (a) shows DSC thermograms of NBDI-, IPDI-, HMDI- and HDI-based hard segment models. NBDI- and IPDI-based HSs model did not show characteristic changes, whereas HMDI- and HDI-based HS models showed exothermic peaks at around 160 and 180 °C, respectively. These can be ascribed to melting of crystallized molecules. Therefore, it seems reasonable to conclude that the NBDI- and IPDI-based HS model can not crystallize, while HMDI- and HDI-based HS models can crystallize. Furthermore, the crystal state of the hard segment models was evaluated by WAXD measurement. As one can see in Fig. 2, HMDI- and HDI-based HS models exhibited crystalline peaks which are from interchain distances. Intensity of crystalline peaks of HMDI-based HS is quite weak, indicating that this model includes a lot of amorphous component. This would be related to existence of various types of isomers in case of HMDI. Figure 3 (a) and (b) shows stress-strain curves and temperature dependence of dynamic viscoelastic functions (dynamic storage modulus (*E'*), dynamic loss modulus (*E''*) and loss tangent (tan δ)) of NBDI-, IPDI-, HMDI- and HDI-based PUs. Note that the samples shown in Fig. 3 are not HS models but elastomers. Poly(oxytetramethylene) glycol (PTMG) and BD were used as a soft segment component and chain extender, respectively, for these elastomers. NBDI- and IPDI-based PU showed lower Young's modulus and tensile strength in

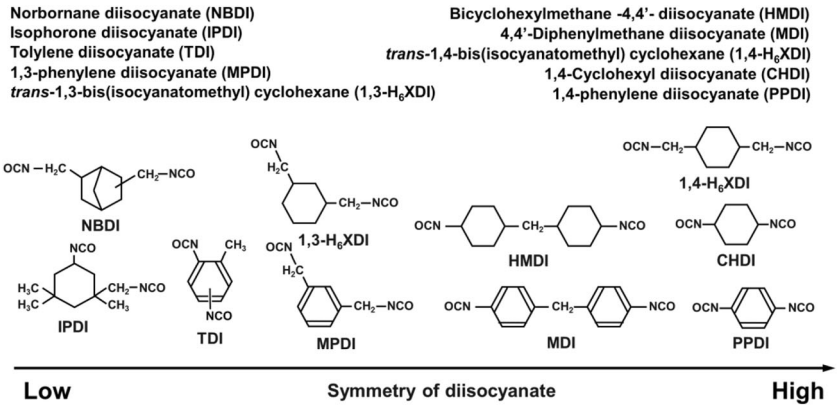

Fig. 1 Chemical structure and symmetry of diiscocyanates shown in the review

comparison with HMDI- and HDI-based PU. This trend corresponds to the *E'* at the rubbery plateau regionas shown in Fig. 3 (b). Lower aggregation force of NBDI- and IPDI-based PU induces low degree of microphase separation, resulting in absence of physical cross-linking domains, which can keep applied force during mechanical deformation. The *E'* value of all PUs gradually decreased at around −70 °C, which may be due to glass transition of purer PTMG chains. For NBDI-, IPDI-, and HMDI-based PUs, the *E'* value decreased at 50 °C, which is associated with the glass transition of a mixed phase with soft and hard segment chains. Further, the HDI-based PU showed larger *E'* value at the rubbery plateau region and the temperature at which terminal flow stated was the highest of the four. This implies that the degree of microphase separation is the strongest and the hard segment chains crystallized with the formation of hydrogen bonds.

Cyclohexane diisocyanate-based PU: effect of hard segment content (HSC)

Most PUs are commercially made from aromatic diisocyanates, MDI and TDI, since these isocyanates are reactive and low cost and can give better mechanical property. A problem of these aromatic diisocyanate-based PUs is low color stability. On the contrary, cycloroaliphatic diisocyanate is expected to produce low-color change PU because it does not have benzene rings, which can be changed to quinone structure with yellow color. However, most of the cycloaliphatic isocyanates has an asymmetric structure, resultant PUs generally have poor mechanical properties due to weaker microphase separation on account of lower aggregation force of hard segment chains. Lin et al. [31, 32] reported hydrogen bonding states of 1,3-H_6XDI based liquid crystalline elastomer using FT-IR. Xie et al. [94] synthesized 1,3- and 1,4-H_6XDI- and IPDI- and HMDI- based PU using polycaprolactone and 1,4-BD and investigated the degree of microphase separation and mechanical properties by temperature dependence of dynamic viscoelastic property measurement and tensile testing. The 1,3- and 1,4-H_6XDI-PU showed lower and narrower glass transition of soft segment at around −40 °C, indicating that the PU possesses stronger degree of microphase separation and better mechanical properties in comparison with IPDI- and HMDI-based PU. This may be due to small, compact, and symmetric structure of 1,3- and 1,4-H_6XDI.

Yamasaki et al. produced new commercial diisocyanate to solve these open questions [39]. Yamasaki and Kojio et al. reported relationship between molecular aggregation structure and mechanical property of resultant PU using SAXS,

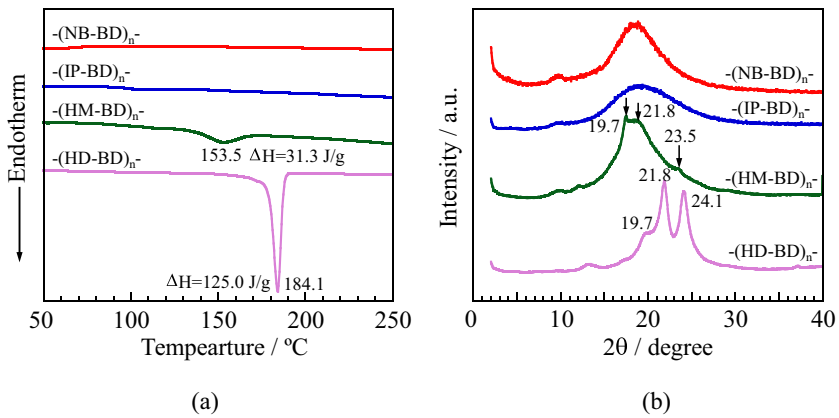

Fig. 2 **a** DSC curves and **b** WAXD profiles of NBDI-, IPDI-, HMDI and HDI-based had segment (HS) models. "-(XX-BD)$_n$-" denotes hard segment models consisting diisocyanate (XX) and 1,4-butanediol (BD) [10]

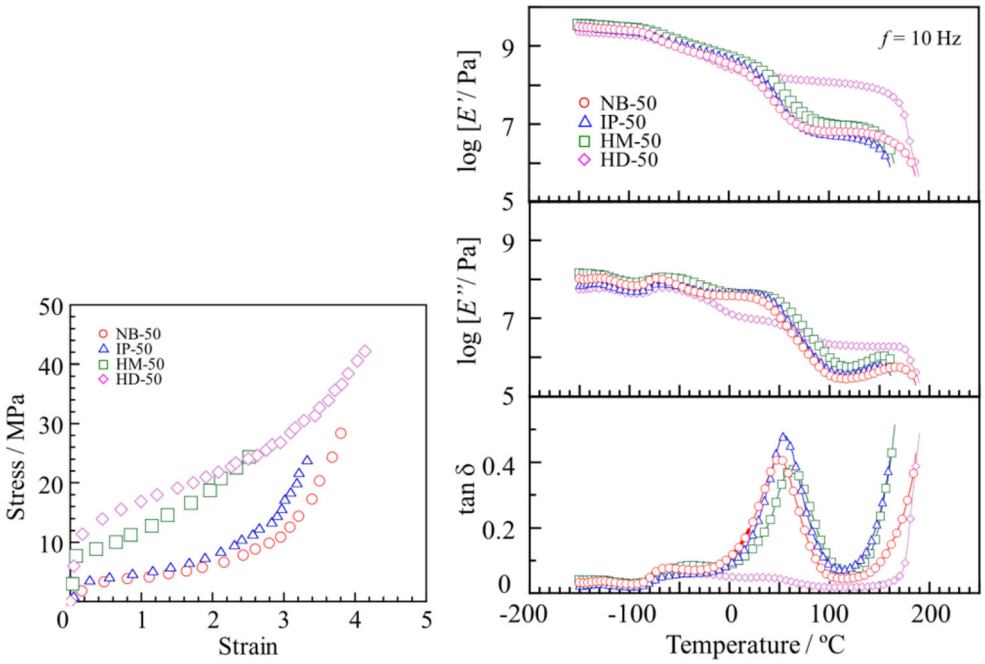

Fig. 3 **a** Stress-strain curves at room temperature and **b** temperature dependence of dynamic storage modulus (E'), dynamic loss modulus (E'') and loss tangent (tan δ) of NBDI-, IPDI-, HMDI and HDI-based PUs measured at 10 Hz. PTMG and BD were used for synthesis and hard segment content (HSC) was 50 wt%. Last two digits correspond to HSC [10].

WAXD, FT-IR, DSC, X-ray adsorption fine structure (XAFS), dynamic viscoelastic property, and tensile test [33, 35, 36, 40, 95]. PTMG and BD were used as raw materials for synthesis of PUs. Hard segment content (HSC) was controlled by changing molar ratio of three components. The last two digit of sample name corresponds to HSC. Figure 4 (a) shows DSC thermograms of 1,4-H_6XDI- and MDI-based PUs with various hard segment contents and hard segment models. MDI was used as a control sample. Abbreviation denotes a type of diisocyanate and hard segment content. HX and MD correspond to 1,4-H_6XDI- and MDI. The T_g of the soft segment chains ($T_{g,S}$) were observed at around −70 °C. 1,4-H_6XDI-based PUs were lower than for MDI-based PUs. The $T_{g,S}$ decreased with an increase in the HSC. Moreover, exothermic peaks observed at 0 °C and 170–210 °C can be assigned to melting of crystallized soft and hard segments ($T_{m,S}$ and $T_{m,H}$), respectively. These $T_{m,S}$ and $T_{m,H}$ decreased and increased with an increase in HSC, indicating that hard segment rich phase was formed at higher HSC. Therefore, it seems reasonable to considered that 1,4-H_6XDI-PTMG-BD-based PU is a strong segregation system. Figure 4 (b) shows WAXD profiles of 1,4-H_6XDI- and MDI-based PUs with various hard segment contents and hard segment models. For the hard segment models of 1,4-H_6XDI and MDI (-(1,4-H_6XDI-BD)$_n$- and

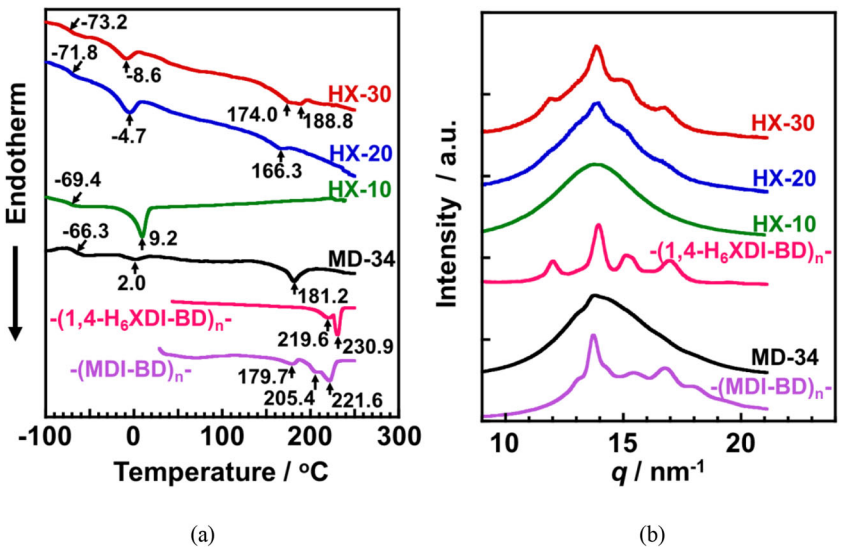

Fig. 4 **a** DSC curves and **b**) WAXD profiles of 1,4-H_6XDI- and MDI-based PUs with various hard segment contents (last two digits) and hard segment models. HX and MD correspond to 1,4-H_6XDI- and MDI [33]

-(MDI-BD)$_n$-), crystalline peaks were clearly observed. The peaks were observed at q = 12.0, 13.9, 15.2 and 17.0 nm^{-1} for 1,4-H$_6$XDI-based model. Based on Rietvelt analysis, the crystal lattice was triclinic, of P1 symmetry, a = 0.759 nm, b = 0.836 nm, c = 1.576 nm, α = 139.3°, β = 139.7°, γ =36.7° [33]. On the other hand, crystalline peaks were observed at q = 13.1, 13.7, 15.4, 16.8 and 18.0 nm^{-1} for MDI-based model. These peak positions correspond to the results for type II crystal reported by Thomas et al. [81], Pompe, et al. [84], Cooper et al. [83], and Kojio et al. [85]. As can be easily seen, crystallinity of 1,4-H$_6$XDI HS model must have had larger value because it is quite hard to recognize amorphous halo for 1,4-H$_6$XDI HS model, in contrast, amorphous halo was clearly detected for MDI-based PU. For both 1,4-H$_6$XDI- and MDI-PU, crystalline peaks were observed at same positions of HS model, indicating that same crystal structure of hard segment domains were formed in the PUs. Even in PU, 1,4-H$_6$XDI-PU-30 exhibited obvious crystalline peaks in comparison with MDI-based PU-34. This result implies that cohesive force of 1,4-H$_6$XDI-BD chains is quite strong, resulting in the formation of well-crystallized hard segment domains.

Next, mechanical properties of the PUs will be given. Figure 5 shows (a) stress-strain curves and (b) dependence of E', E'' and tan δ on temperature of 1,4-H$_6$XDI- and MDI-based PUs. Young's modulus and the E' value at rubbery plateau region of HX-20 and MD-34 were almost comparable, and HX-30 was much larger, even the HSC of HX-30 is lower than for MD-34. This result strongly indicates that the hard segment domains possess well-ordered hard segment domain structure. The HS domains might have been connected each other such as networked structure not like isolated HS domains. Tensile strength of HX-30 was almost comparable with MD-34, though HSC of HX-30 is lower than for MD-34. This result again indicates that the cohesive force of hard segment chains of HX-30 is quite high compared with MD-34. For the 1,4-H$_6$XDI-PU, Young's modulus and tensile strength increased, and elongation at break decreased with an increase in strain. This corresponds to increase in well-developed hard segment domains were formed with an increase in HSC because the 1,4-H$_6$XDI-PU is strong segregation system. In the temperature-E', E'' and tan δ relationship of 1,4-H$_6$XDI- and MDI-based PU, glassy, glass-rubber transition, rubbery plateau, and terminal regions were clearly observed in the temperature range from −150 to 200 °C. Between glass-rubber transition and rubbery plateau region, shoulder was observed at −20 °C. This is associated with recrystallization of the soft segment chains with an increase in temperature. Terminal temperature, which corresponds to heat resistance, was higher for HX-30 and MD-34. These trends were consistent with melting temperature of crystallized hard segment domains obtained by DSC. Cyclic tensile test was conducted for 1,4-H$_6$XDI- and MDI-based PUs as well [33]. Residual strain decreased with an increase in the HSC for 1,4-H$_6$XDI-based PUs. And residual strain of HX-30 was smaller than for MD-34. Therefore, it seems reasonable to conclude that 1,4-H$_6$XDI-based PU showed superior properties compared with MDI-based PUs.

Cyclohexane diisocyanate-based PU: effect of chemical cross-links

Since segmented PUs do not have any chemical cross-linking points but physical cross-linking points, they can show environmental friendly and good recyclable property. However, their mechanical properties are not occasionally sufficient for applications, for example, stress values at various strains, elongation at break, and permanent set. In order to compensate for these requirements, chemical cross-linking points are

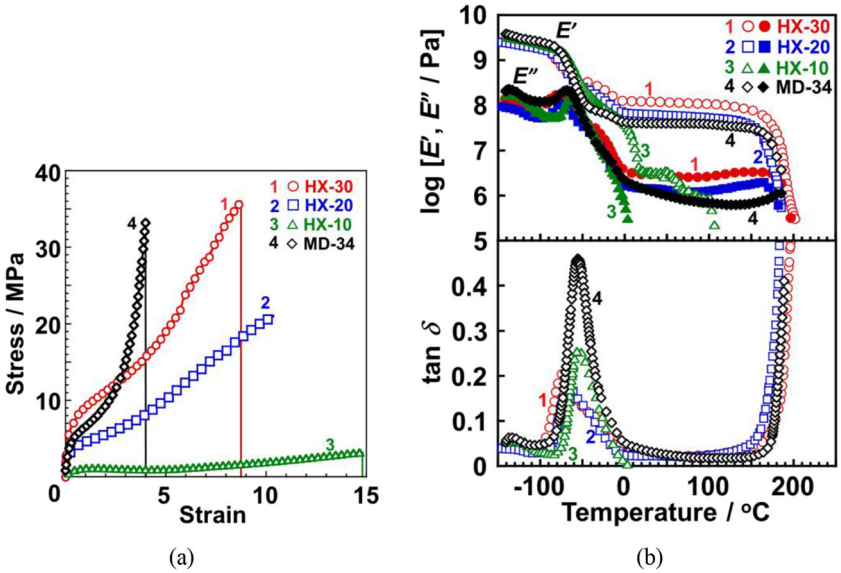

Fig. 5 **a** Stress-strain curves at room temperature and **b** temperature dependence of E', E'' and tan δ of 1,4-H$_6$XDI- and MDI-based PUs with various hard segment contents [33]

positively incorporated [8, 9, 77, 85, 96–99]. There are two main ways to incorporate chemical cross-linking points to PU. One is the using triol, such as poly(oxypropylene) triol, instead of diol. The other one is low molecular weight triol, like 1,1,1-trimehylol propane (TMP), incorporating into hard segment moiety. Petrovic et al. [96] reported that effect of cross-linking points on mechanical properties of PU using poly(oxypropylene) (PPO) and poly(oxypropylene/oxyethylene) triol, MDI, and BD at a constant concentration of hard segments equal 50 wt%. All PU exhibited the two-phase microphase-separated structure. Tensile strength and strain at break increased, while tear strength, hardness, and T_g of soft segment did not change with an increase in the density of chemical cross-linking. Furthermore, the rate of stress relaxation depends on both elongation and the density of chemical cross-linking. Petrovic et al. [97] also reported that mechanical properties of PU elastomers containing chemical cross-links in the hard segment, for PPO with $M_n = 2000$, MDI, BD/TMP-based PUs. The density of chemical cross-linking of the PUs was varied by BD/TMP ratio in the cross-linking agent. With an increase in the density of chemical cross-linking, tensile strength, elongation at break permanent set decreased and breadth of T_g for the soft segment increased.

The authors also clarified effect of incorporation of TMP into hard segment on crystallization behavior of soft segment chains, changes in the structure of hard segment domains, and mechanical properties during the elongation process for PTMG with $M_n = 2000$, MDI, BD/TMP-based PUs. The ratio of BD/TMP was varied from 100/0 to 75/25 [9, 18, 77, 99, 100]. Strain-induced crystallization of PTMG was clearly observed in the ratio range. Incorporation of TMP induced decrease in crystallinity of PTMG soft segment chains and large change in spacing of hard segment domains during the elongation process. Chemical cross-links seemed to reduce the arrangement and ordering of the soft segment chains and to progress application of stress to the whole network structure.

We reported the effect of incorporation of TMP into PTMG-1,4-H_6XDI-BD-based PUs. Figure 6 (a) shows DSC thermograms of 1,4-H_6XDI-based PUs with various 1,4-BD/TMP ratios and HSCs. As one can see, $T_{g,S}$, $T_{m,S}$, and $T_{m,H}$ were clearly observed at around −70, 0, and 170 °C, respectively. As stated in previous section, $T_{g,S}$ and $T_{m,S}$ decreased and $T_{m,H}$ increase with increasing HSC. On the other hand, all $T_{g,S}$ and $T_{m,S}$, and $T_{m,H}$ increased with an increase in the TMP ratio. These results indicate that the purities of the soft segment phase and the crystallized hard segment domains slightly decreased and increased, respectively. The incorporation of TMP might have progressed crystallization of the hard segment chains because 1,4-H_6XDI-BD-based hard segment chains with strong cohesive force among them were properly disconnected [9, 100]. This phenomenon is similar to the change in melting temperature for controlled length of MDI-BD crystal [101, 102]. Figure 6 (b) shows WAXD profiles of 1,4-H_6XDI-based PUs with various 1,4-BD/TMP ratios and HSCs. The peaks of crystallized hard segment domains were observed for all PUs. Incorporation of TMP decreased the peak intensity. This is reasonable because the TMP molecules are directly connected to isocyanate end groups of prepolymer molecules.

Figure 7 shows (a) stress-strain curves and (b) dependence of E', E'' and tan δ on temperature of 1,4-H_6XDI-based PU with various BD/TMP ratio and HSCs. Young's modulus of HX-30-10/0, HX30–8/2, HX-20-10/0, and HX20–8/2 were 19.1, 11.4, 8.0, and 6.1 MPa, respectively. Since the incorporation of TMP induces restriction of aggregation of the hard segment chains as clarified DSC and WAXD results, decreasing Young's modulus seems to be valid. On the contrary, tensile strength and strain at break of HX-30-10/0, HX30–8/2, HX-20-10/0, HX20–8/2 were 36.3, 37.4, 18.5, 20.7 MPa, and 8.8, 5.0, 14.5, 6.1, respectively. As shown in stress-strain curves, slope at the high strain region for HX30–8/2 and HX-20-8/2 were quite large in comparison with HX30–10/0, HX-20-10/0, in other words, obvious upturn was observed. This is simply associated with increasing density of cross-linking points. The reason that tensile strength and strain at break decrease with incorporation of TMP might be due to decrease in hard segment domains, which can work as a filler, and increase in inhomogeneity of network structure. As shown in Fig. 7 (b), the temperature, at which glass transition of the soft segment chains occurs, shoulders right after the glass transition, and the E' magnitude at rubbery plateau region, correspond well to data obtained by DSC and tensile testing. The terminal temperature of HX30–8/2 and HX-20-8/2 were obviously higher than for HX30–10/0 and HX-20-10/0. Furthermore, above terminal temperature, the E' magnitude of HX30–10/0 and HX-20-10/0 simply decreased, in contrast, that for HX30–8/2 and HX-20-8/2 showed shoulders above the temperature. This must be related to chemical cross-linking points formed by TMP.

Cyclohexane diisocyanate-based thiourethane

Thiourethane can be obtained by a reaction between isocyanate and thiol groups. Thiourethane has different properties with urethane groups, some researches have been performed. Li et al. [103] synthesized regular urethane, thiourethane, and dithiourethane compounds as a hard segment model and then investigated their hydrogen bond strengths. The strengths for urethane groups and thiourethane groups are similar, in contrast, that for dithiourethane is lower than the other two. Furthermore, they suggest that the hydrogen bond strength and the structure of diisocyanate influence the mechanical properties of, polythiourethane, and polydithiourethane. Shin et al. [104] reported the effect of the molecular weight of hard

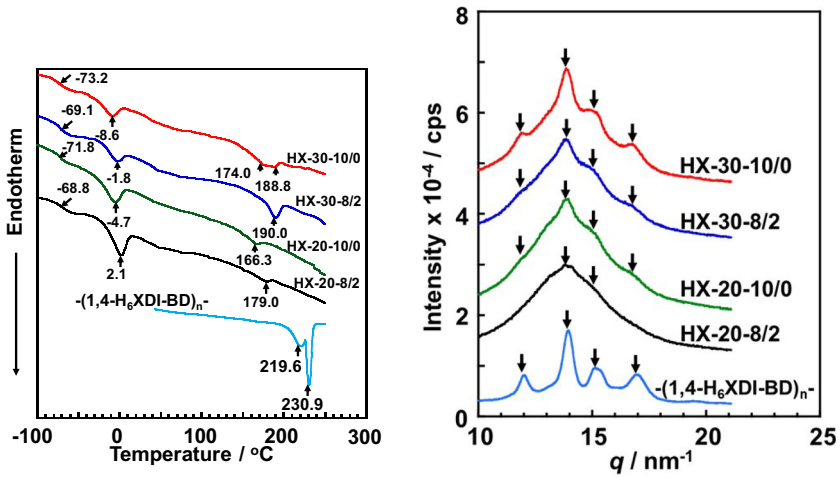

Fig. 6 **a** DSC curves and **b** WAXD profiles of 1,4-H_6XDI-based PUs with various hard segment contents and TMP contents [40]

and soft segments and their ratio, and the chemical structure of hard segment on phase separation and mechanical properties of polythiourethanes (PTUs). They clarified that factors mentioned above influenced on Young's modulus, elongation at break and tensile strength.

We have recently reported the influence of chain extender, dithiol and diol, on the molecular aggregation structure and mechanical properties [35]. Figure 8 shows (a) DSC thermograms of 1,4-H_6XDI-PTMG-based TPUs synthesized with 1,4-butanediol (BD), 1,5-pentanediol (PD), 1,4-butanedithiol (BDT), 1,5-pentanedithiol (PDT). Shifts of baseline and exothermic and two endothermic peaks were observed at around −72, −30, 0, and 160 °C, respectively. They are assigned to glass transition, recrystallization, melting of soft segment chains and melting of the crystallized hard segment domains, respectively. The $T_{g,S}$s of PTUs were lower than for PUs. And T_gs of the C4 chain extender, BD and BDT-based elastomers showed lower than C5 chain extender-based elastomer. ($T_{m,\,H}$) of C4 and diol chain extender-based elastomers showed higher temperature. Figure 8 (b) shows WAXD profiles of 1,4-H_6XDI-PTMG-based TPUs synthesized with BD, PD, BDT, or PDT. C4 and diol chain extender-based HS model exhibited sharper crystalline peaks. This trend corresponds well to $T_{m,\,H}$ shown in DSC curves of Fig. 8 (a). Therefore, it seems reasonable from DSC measurements to conclude that the degree of microphase separation in C4 chain extender-based elastomers (PTU-B and PU-B) is stronger than for C5 one (PTU-P and PU-P), and degree of microphase separation of thiol-based elastomer (PTU-B and PTU-P) is stronger than for diol-based elastomers (PU-B and PU-P). In other words, PTU-B possesses the strongest degree of microphase separation of the four.

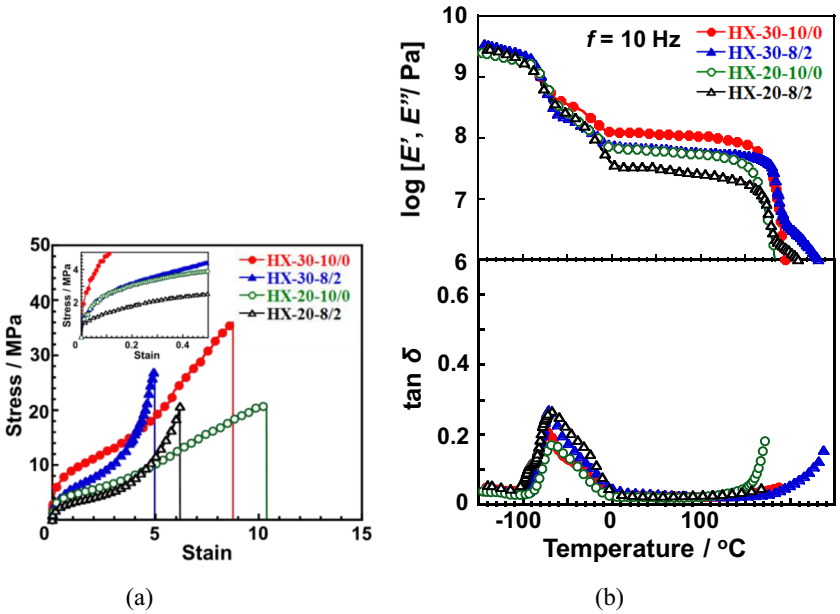

Fig. 7 **a** Stress-strain curves at room temperature and **b** temperature dependence of E', E'' and tan δ of 1,4-H_6XDI-based PUs with various hard segment contents and TMP contents [40]

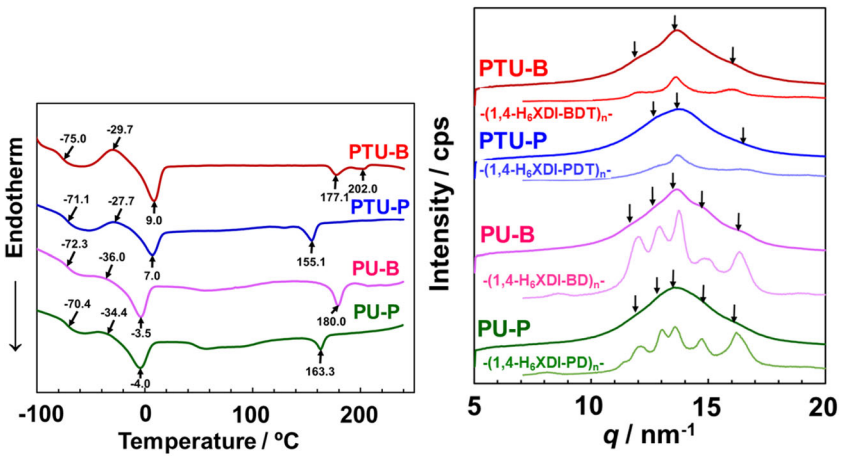

(a) (b)

Fig. 8 **a** DSC curves and **b** WAXD profiles of 1,4-H_6XDI-PTMG-based TPUs synthesized with BD, PD, BDT, or PDT

Generally speaking, PU elastomers with the strong degree of microphase separation exhibit superior mechanical property. This is because each pure phase can show the best required properties, for example, low T_g of the soft segment chains, and high T_m of hard segment chains. The high T_m of hard segment chains gives high heat resistance, Young's modulus and tensile strength on account of robust connectivity between hard segment domains. Mechanical property was investigated for PTU and PU elastomers by tensile testing and dynamic viscoelastic property measurement. Figure 9 shows (a) stress-strain curves and (b) temperature dependence of *E'*, *E''* and tan δ of 1,4-H_6XDI-PTMG-based TPUs synthesized with BD, PD, BDT, or PDT. Young's modulus obtained by an initial slope of stress-strain curves for four elastomers was following order: PU-B > PTU-B > PU-P > PTU-P. Moreover, tensile strength was following order: PU-B > PTU-B ≒ PU-P ≒ PTU-P. Thus, mechanical properties did not follow the degree of microphase separation in these PU and PTU systems. The reason that the PU-B showed the largest mechanical property is that the formation of robust hard segment domains by strong cohesive force among the hard segment chains. On the other hand, though PTU-B has the strongest microphase separation, robustness of the hard segment domains seems not to be high enough. This can be inferred from broad and weak crystalline peaks as shown in WAXD profile (Fig. 8 (b)). PTU-P exhibited the lowest mechanical property due to the lowest degree of microphase separation and low cohesive force among hard segment chains. PU-P also showed lower mechanical property in comparison with PU-B, indicating that 1,4-H_6XDI and PDT or PD is not good combination in terms of cohesive force of the hard segment chains. In the temperature dependence of *E'*, *E''* and tan δ of 1,4-H_6XDI-PTMG-based TPUs, the ordering of the *E'* values at the rubbery plateau region followed those of Young's modulus. In the terminal flow region, PTU-B exhibited gradual decrease at 130 °C, which is lower than for PU-B, although the $T_{m,H}$ of PTU-B is higher than for PU-B. This implies that low cohesive force of the hard segment chains of PTU-B.

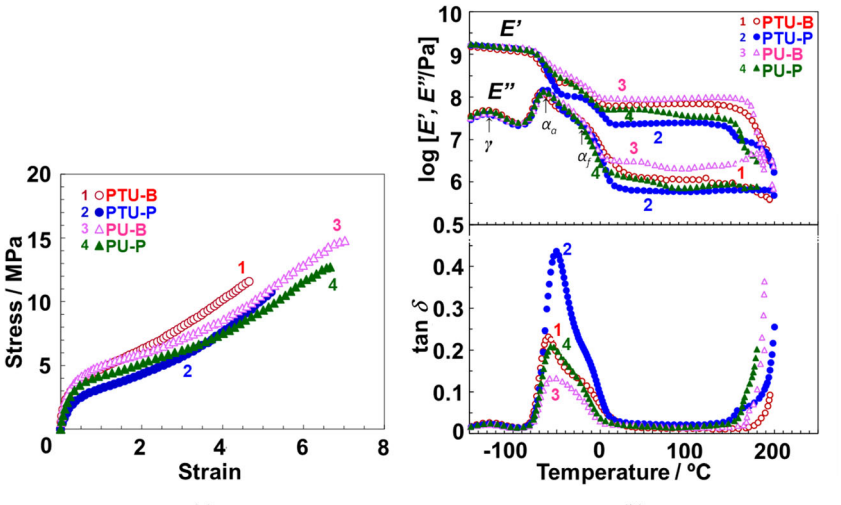

(a) (b)

Fig. 9 **a** Stress-strain curves at room temperature and **b** temperature dependence of *E'*, *E''* and tan δ of 1,4-H_6XDI-PTMG-based TPUs synthesized with BD, PD, BDT, or PDT

In situ investigation of structure during mechanical deformation

In situ molecular aggregation structure analysis of the materials is quite important. Especially, in the case of the polymeric materials, deformation behavior is quite sensitive to time because of relaxation behavior, in situ analysis is indispensable to understand the relationship between molecular aggregation structure and mechanical properties. X-ray analysis [74, 76, 105], Fourier transformed infrared spectroscopy [69, 70], birefringence measurements [106–108] can be given as the experimental methods of in situ molecular aggregation structure analysis. Figure 10 (a) shows 2D-SAXS patterns of PTU-B at various strains, (b) 1D-SAXS profiles along meridional and equatorial directions, and (c) azimuthal profiles of 2D-SAXS patterns at $q = 0.26–0.33$ nm^{-1}. Isotropic ring pattern corresponding to spacing among hard segment domains was observed at the initial state ($\varepsilon = 0$, A peak shown in Fig. 10 (b)). With increasing strain, four-point patterns were observed at strain of 0.3~0.5. This change is associated with the formation of zig-zag structure of hard segment domains. With further increase in strain, triangle scattering was observed upper and lower sides of the beam stopper. These correspond to compressed and stepped aligned hard segment domains perpendicular to the stretching direction. The streak observed at the equatorial line implies that the formation of bundles along the stretching direction. As shown in Fig. 10 (b), the peak from domain spacing shifted to low and high q region along parallel and perpendicular direction to stretching direction. To discuss these results more quantitatively, strain obtained from domain spacing was plotted for PTU-B and PTU-P. Figure 11 shows relationship between film strain and strain obtained from spacing of hard segment domains ($\Delta d/d$) for PTU-B and PTU-P obtained from 1D-SAXS profiles in the strain range from 0 to 4. Domain spacing was calculated using three-dimensional correlations functions. Both PTU-B and PTU-P showed smaller $\Delta d/d$ magnitude in comparison with film strain. In the larger strain region of 1.5, the $\Delta d/d$ magnitude of PTU-B was constant, in contrast, $\Delta d/d$ magnitude of PTU-P showed maximum at around strain of 1.5, and recovered almost to initial value. These results clearly indicate that the cohesive force of thiourethane groups are quite weak. Even if domain spacing returned to initial value at strain of 3.5, the large stress was observed in the stress-strain curves as shown in Fig. 9 (a), indicating that recombination between hard segment chains may have occurred during the elongation process.

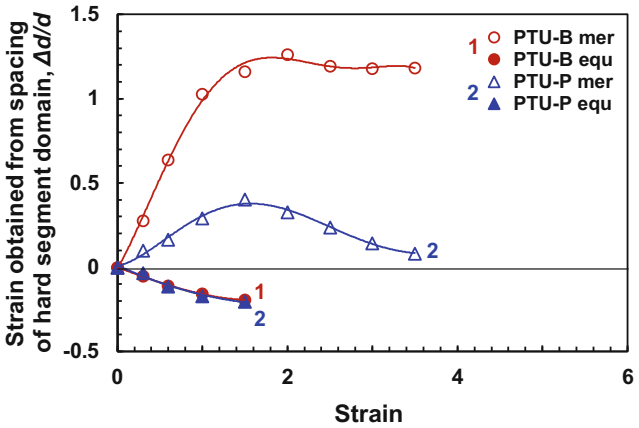

Fig. 11 Relationship between film strain and strain obtained from spacing of hard segment domains, $\Delta d/d$ for PTU elastomers obtained from 1D-SAXS profiles at various strains, calculated using three-dimensional correlations functions

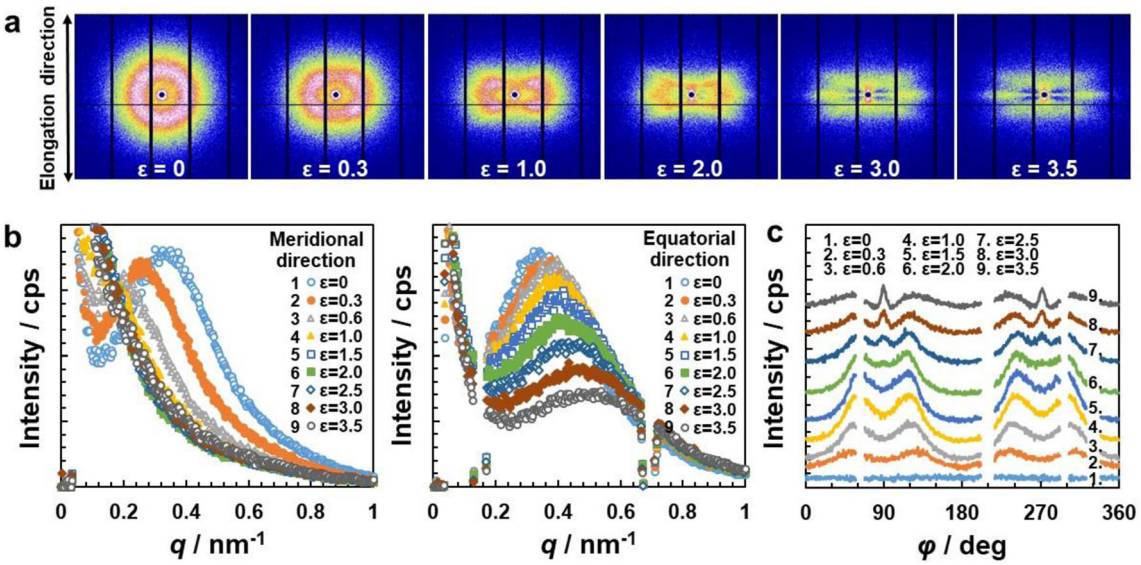

Fig. 10 **a** 2D-SAXS patterns of PTU-B at various strains. **b** 1D-SAXS profiles along meridional and equatorial directions, and **c** azimuthal profiles of 2D-SAXS patterns at $q = 0.26–0.33$ nm^{-1}

Conclusions

In this review, structure-property relation of cycloaliphatic diisocyanate-based PUs were introduced. IPDI, NBDI, TDI, 1,3-H_6XDI, MPDI, HMDI, MDI, 1,4-H_6XDI, CHDI, and PPDI based PU were synthesized with PTMG and BD and their molecular aggregation structures and properties were investigated. Bulky and asymmetric isocyanate, NBDI, IPDI, and TDI-based PUs showed lower degree of microphase separation and mechanical properties. With increase in symmetry of diisocyanate, both degree of microphase separation and mechanical properties became better. This is because symmetric structure induces formation of hydrogen bond and crystallization. Controls of hard segment content and chemical crosslinking density work well to change mechanical properties of PUs. Concrete results of these controls were explained using PTMG-1,4-H_6XDI-BD/TMP-based PU. Polythiourethane showed stronger microphase separation but weaker mechanical properties in comparison with polyreuthane. This is because weak cohesive force of the thiourethane segments chains in the elastomers. In situ SAXS/WAXD measurement revealed that formation of a zig-zag structure of hard segment domains and bundle structure at high strain. Strain obtained from SAXS results for PTU-P was much smaller than for PTU-B due to weak cohesive force of C5 chains.

Acknowledgements The authors greatly appreciate Miss Shiori Masuda, Dr. Rahmawati, Dr. Kazutaka Kamitani, Dr. Naoki Shinohara, Mr. Kiminori Uchida, Dr. Kazuki Mita for their experimental supports. This work was supported by the Impulsing Paradigm Change through Disruptive Technology (ImPACT) Program, the Photon and Quantum Basic Research Coordinated Development Program from the Ministry of Education, Culture, Sports, Science and Technology, Japan. In situ simultaneous SAXS/WAXD measurements were conducted at the BL03XU and BL40XU Spring-8 facility with the approval of the Japan Synchrotron Radiation Research Institute (JASRI; Proposal No. 2012B1506, 2013B1186, 2014B1198, 2014B7266, 2015A1514, 2015A7216, 2015B7267, 2016A7217, 2016B7266, 2017A7215, 2017B7267, 2018A7217, and 2018B 7267). We gratefully acknowledge Dr. Hiroyasu Masunaga and Dr. Taizo Kabe (JASRI), for their assistance on the SAXS and WAXD measurements.

References

1. Pigott KA, Frye BF, Allen KR, Steingiser SS, Darr WC, Saunders JH, Hardy EE (1960) Development of cast urethane elastomers for ultimate properties. J Chem Eng Data 5:391–395. https://doi.org/10.1021/je60007a044
2. Saunders JH, Frisch KC (1962) Polyurethanes: chemistry and technology, part 1, chemistry. Wiley, New York
3. Cooper SL, Tobolsky AV (1966) Properties of linear elastomeric polyurethanes. J Appl Polym Sci 10:1837–1844. https://doi.org/10.1002/app.1966.070101204
4. Kajiyama T, Macknight WJ (1969) Low-temperature relaxations in Polyurethans. Macromolecules 2:254–261. https://doi.org/10.1021/ma60009a009
5. Petrovic ZS, Ferguson J (1991) Polyurethane elastomers. Prog Polym Sci 16:695–836. https://doi.org/10.1016/0079-6700(91)90011-9
6. Hepburn C (1992) Polyurethane elastomers, 2nd edn. Elsevier Applied Science, Ltd.
7. Cooper SL, Tobolsky AV (1966) Viscoelastic behavior of segmented elastomers. Textile Research Journal 36:800. https://doi.org/10.1177/004051756603600905
8. Kojio K, Fukumaru T, Furukawa M (2004) Highly softened polyurethane elastomer synthesized with novel 1,2-bis(isocyanate)ethoxyethane. Macromolecules 37:3287–3291. https://doi.org/10.1021/ma0359988
9. Kojio K, Nakamura S, Furukawa M (2004) Effect of side methyl groups of polymer glycol on elongation-induced crystallization behavior of polyurethane elastomers. Polymer 45:8147–8152. https://doi.org/10.1016/j.polymer.2004.09.061
10. Kojio K, Nakashima S, Furukawa M (2007) Microphase-separated structure and mechanical properties of norbornane diisocyanate-based polyurethanes. Polymer 48:997–1004. https://doi.org/10.1016/j.polymer.2006.12.057
11. Kojio K, Uchiba Y, Mitsui Y, Furukawa M, Sasaki S, Matsunaga H, Okuda H (2007) Depression of microphase-separated domain size of polyurethanes in confined geometry. Macromolecules 40:2625–2628. https://doi.org/10.1021/ma0700577
12. Yamasaki S, Nishiguchi D, Kojio K, Furukawa M (2007) Effects of aggregation structure on rheological properties of thermoplastic polyurethanes. Polymer 48:4793–4803. https://doi.org/10.1016/j.polymer.2007.06.006
13. Barikani M, Hepburn C (1987) The relative thermal stability of polyurethane elastomers: effect of diisocyanate structure. Cell Polym 6:41–54
14. Yamasaki S, Nishiguchi D, Kojio K, Furukawa M (2007) Effects of polymerization method on structure and properties of thermoplastic polyurethanes. J Polym Sci B Polym Phys 45:800–814. https://doi.org/10.1002/polb.21080
15. Casetta C, Girelli D, Greco A (1994) Pitture e Vernici Europe 70:9–16
16. Kojio K, Nonaka Y, Masubuchi T, Furukawa M (2004) Effect of the composition ratio of copolymerized poly(carbonate) glycol on the microphase-separated structures and mechanical properties of polyurethane elastomers. J Polym Sci B Polym Phys 42:4448–4458. https://doi.org/10.1002/polb.20303
17. Kojio K, Furukawa M, Motokucho S, Shimada M, Sakai M (2009) Structure−mechanical property relationships for poly(carbonate urethane) elastomers with novel soft segments. Macromolecules 42:8322–8327. https://doi.org/10.1021/ma901317t
18. Kojio K, Furukawa M, Nonaka Y, Nakamura S (2010) Control of mechanical properties of thermoplastic polyurethane elastomers by restriction of crystallization of soft segment. Materials 3:5097–5110. https://doi.org/10.3390/ma3125097
19. Kojio K, Furukawa M, Shimada M, Shimada M, Komatsu T, Nozaki S, Motokucho S, Yoshinaga K (2015) Improvement of the low-temperature property of aliphatic polycarbonate glycols-based polyurethane elastomers. Sci Adv Mater 7:934–939. https://doi.org/10.1166/sam.2015.1913
20. Špírková M, Pavličević J, Strachota A, Poreba R, Bera O, Kaprálková L, Baldrian J, Šlouf M, Lazić N, Budinski-Simendić J (2011) Novel polycarbonate-based polyurethane elastomers: composition–property relationship. Eur Polym J 47:959–972. https://doi.org/10.1016/j.eurpolymj.2011.01.001
21. Pavličević J, Špírková M, Jovičić M, Bera O, Poręba R, Budinski-Simendić J (2013) The structure and thermal properties of novel polyurethane/organoclay nanocomposites obtained by pre-polymerization. Compos Part B 45:232–238. https://doi.org/10.1016/j.compositesb.2012.09.018

22. Eceiza A, Martin MD, de la Caba K, Kortaberria G, Gabilondo N, Corcuera MA, Mondragon I (2008) Thermoplastic polyurethane elastomers based on polycarbonate diols with different soft segment molecular weight and chemical structure: mechanical and thermal properties. Polym Eng Sci 48:297–306. https://doi.org/10.1002/pen.20905
23. Kojio K, Furukawa M, Motokucho S, Mizokami M, Yoshinaga K (2012) Influence of side group contents of polycarbonate glycol on aggregation structures and mechanical properties of polyurethane elastomers. Nippon Gomu Kyokaishi 85:151–156. https://doi.org/10.2324/gomu.85.151
24. Lambert R, Ibarboure E, Fleury G, Carlotti S (2019) Low-temperature amino-based catalyst activation for on-demand polyurethane synthesis. Polym J. https://doi.org/10.1038/s41428-019-0246-8
25. Zhang Y, Qi YH, Zhang ZP (2015) The influence of 2,4-toluene diisocyanate content on the intrinsic self-healing performance of polyurethane at room-temperature. J Polym Res 22:94. https://doi.org/10.1007/s10965-015-0744-0
26. Takahara A, Tashita J, Kajiyama T, Takayanagi M, Macknight WJ (1985) Microphase separated structure, surface-composition and blood compatibility of segmented poly(urethaneureas) with various soft segment components. Polymer 26:987–996. https://doi.org/10.1016/0032-3861(85)90218-6
27. Higaki Y, Suzuki K, Oniki Y, White KL, Ohta N, Takahara A (2015) Molecular aggregation structure evolution during stretching of environmentally benign lysine-based segmented poly(urethane-urea)s. Polymer 78:173–179. https://doi.org/10.1016/j.polymer.2015.10.002
28. Oprea S, Timpu D, Oprea V (2019) Design-properties relationships of polyurethanes elastomers depending on different chain extenders structures. J Polym Res 26:117. https://doi.org/10.1007/s10965-019-1777-6
29. Nakagawa T, Takeuchi H, Sato K, Yamasaki S (2016) Pentamethylene diisocyanate. US patent US 9,376,404 B2,
30. Hespe HF, Zembrod A, Cama FJ, Lantman CW, Seneker SD (1992) Influence of molecular-weight on the thermal and mechanical-properties of polyurethane elastomers based on 4,4′-diisocyanato dicyclohexylmethane. J Appl Polym Sci 44:2029–2035. https://doi.org/10.1002/app.1992.070441118
31. Lin CK, Kuo JF, Chen CY (2000) Synthesis and mesomorphism of thermotropic liquid crystalline polyurethanes based on meta-diisocyanates with 4,4 '-bis(omega-hydroxyalkoxy) biphenyls. Eur Polym J 36:1183–1193. https://doi.org/10.1016/s0014-3057(99)00164-0
32. Lin C-K, Kuo JF, Chen CY, Fang J-J (2012) Investigation of bifurcated hydrogen bonds within the thermotropic liquid crystalline polyurethanes. Polymer 53:254–258. https://doi.org/10.1016/j.polymer.2011.11.009
33. Nozaki S, Masuda S, Kamitani K, Kojio K, Takahara A, Kuwamura G, Hasegawa D, Moorthi K, Mita K, Yamasaki S (2017) Superior properties of polyurethane elastomers synthesized with aliphatic diisocyanate bearing a symmetric structure. Macromolecules 50:1008–1015. https://doi.org/10.1021/acs.macromol.6b02044
34. Yamasaki S, Kuwamura G, Morita H, Hasegawa D, Kojio K, Takahara A (2017) High performance polyurethane elastomers using new cyclaliphatic diisocyanate. Nihon Reoroji Gakkaishi 45:261–268
35. Rahmawati R, Nozaki S, Kojio K, Takahara A, Shinohara N, Yamasaki S (2019) Microphase-separated structure and mechanical properties of cycloaliphatic diisocyanate-based thiourethane elastomers. Polym J 51:265–273. https://doi.org/10.1038/s41428-018-0148-1
36. Rahmawati R, Masuda S, Cheng C-H, Nagano C, Nozaki S, Kamitani K, Kojio K, Takahara A, Shinohara N, Mita K, Uchida K, Yamasaki S (2019) Investigation of deformation behavior of thiourethane elastomers using in situ X-ray scattering, diffraction, and absorption methods. Macromolecules 52:6825–6833
37. Yilgor I, Yilgor E, Guler IG, Ward TC, Wilkes GL (2006) FTIR investigation of the influence of diisocyanate symmetry on the morphology development in model segmented polyurethanes. Polymer 47:4105–4114. https://doi.org/10.1016/j.polymer.2006.02.027
38. Yilgör I, Yilgör E, Wilkes GL (2015) Critical parameters in designing segmented polyurethanes and their effect on morphology and properties: a comprehensive review. Polymer 58:A1–A36. https://doi.org/10.1016/j.polymer.2014.12.014
39. Kuwamura G, Nakagawa T, Hasegawa D, Yamasaki S (2009) Bis(isocyanatomethyl)cyclohexane for making polyurethane resin useful for various applications. WO2009051114A1,
40. Kojio K, Nozaki S, Takahara A, Yamasaki S (2019) Control of mechanical properties of polyurethane elastomers synthesized with aliphatic diisocyanate bearing a symmetric structure. Elastomers and Composites 54:271–278. https://doi.org/10.7473/ec.2019.54.4.271
41. Kihara N, Endo T (1993) Synthesis and properties of poly(Hydroxyurethane)s. J Polym Sci, Part A: Polym Chem 31:2765–2773. https://doi.org/10.1002/pola.1993.080311113
42. Tomita H, Sanda F, Endo T (2001) Model reaction for the synthesis of polyhydroxyurethanes from cyclic carbonates with amines: substituent effect on the reactivity and selectivity of ring-opening direction in the reaction of five-membered cyclic carbonates with amine. J Polym Sci, Part A: Polym Chem 39:3678–3685. https://doi.org/10.1002/pola.10009
43. Tomita H, Sanda F, Endo T (2001) Structural analysis of polyhydroxyurethane obtained by polyaddition of bifunctional five-membered cyclic carbonate and diamine based on the model reaction. J Polym Sci, Part A: Polym Chem 39:851–859. https://doi.org/10.1002/1099-0518(20010315)39:6<851::aid-pola1058>3.0.co;2-3
44. Leitsch EK, Beniah G, Liu K, Lan T, Heath WH, Scheidt KA, Torkelson JM (2016) Nonisocyanate thermoplastic Polyhydroxyurethane elastomers via cyclic carbonate Aminolysis: critical role of hydroxyl groups in controlling Nanophase separation. ACS Macro Lett 5:424–429. https://doi.org/10.1021/acsmacrolett.6b00102
45. Beniah G, Chen X, Uno BE, Liu K, Leitsch EK, Jeon J, Heath WH, Scheidt KA, Torkelson JM (2017) Combined effects of carbonate and soft-segment molecular structures on the Nanophase separation and properties of segmented Polyhydroxyurethane. Macromolecules 50:3193–3203. https://doi.org/10.1021/acs.macromol.6b02513
46. Beniah G, Fortman DJ, Heath WH, Dichtel WR, Torkelson JM (2017) Non-Isocyanate polyurethane thermoplastic elastomer: amide-based chain extender yields enhanced Nanophase separation and properties in Polyhydroxyurethane. Macromolecules 50:4425–4434. https://doi.org/10.1021/acs.macromol.7b00765
47. Yuan XK, Sang ZH, Zhao JB, Zhang ZY, Zhang JY, Cheng J (2017) Synthesis and properties of non-isocyanate aliphatic thermoplastic polyurethane elastomers with polycaprolactone soft segments. J Polym Res 24:88. https://doi.org/10.1007/s10965-017-1249-9
48. Lai S-M, Wu W-L, Wang Y-J (2016) Annealing effect on the shape memory properties of polylactic acid (PLA)/thermoplastic polyurethane (TPU) bio-based blends. J Polym Res 23:99. https://doi.org/10.1007/s10965-016-0993-6
49. Liff SM, Kumar N, McKinley GH (2007) High-performance elastomeric nanocomposites via solvent-exchange processing. Nat Mater 6:76–83. https://doi.org/10.1038/nmat1798
50. Tien YI, Wei KH (2001) High-tensile-property layered silicates/polyurethane Nanocomposites by using reactive silicates as

Pseudo chain extenders. Macromolecules 34:9045–9052. https://doi.org/10.1021/ma010551p
51. Higaki Y, Otsuka H, Endo T, Takahara A (2003) Polyurethane macroinitiator for controlled monomer insertion of styrene. Macromolecules 36:1494–1499. https://doi.org/10.1021/ma021091i
52. Otsuka H, Aotani K, Higaki Y, Takahara A (2003) Polymer scrambling: macromolecular radical crossover reaction between the main chains of alkoxyamine-based dynamic covalent polymers. J Am Chem Soc 125:4064–4065. https://doi.org/10.1021/ja0340477
53. Ghosh B, Urban MW (2009) Self-repairing oxetane-substituted chitosan polyurethane networks. Science 323:1458–1460. https://doi.org/10.1126/science.1167391
54. Amamoto Y, Otsuka H, Takahara A, Matyjaszewski K (2012) Self-healing of covalently cross-linked polymers by reshuffling thiuram disulfide moieties in air under visible light. Adv Mater 24:3975–3980. https://doi.org/10.1002/adma.201201928
55. Oku T, Furusho Y, Takata T (2004) A concept for recyclable cross-linked polymers: topologically networked polyrotaxane capable of undergoing reversible assembly and disassembly. Angew Chem Int Ed Engl 43:966–969. https://doi.org/10.1002/anie.200353046
56. Murakami H, Nishiide R, Ohira S, Ogata A (2014) Synthesis of MDI and PCL-diol-based polyurethanes containing 2 and 3 rotaxanes and their properties. Polymer 55:6239–6244. https://doi.org/10.1016/j.polymer.2014.10.003
57. Kim BK, Lee JC (1996) Waterborne polyurethanes and their properties. J Polym Sci, Part A: Polym Chem 34:1095–1104. https://doi.org/10.1002/(sici)1099-0518(19960430)34:6<1095::aid-pola19>3.0.co;2-2
58. Kim BK, Seo JW, Jeong HM (2003) Morphology and properties of waterborne polyurethane/clay nanocomposites. Eur Polym J 39:85–91. https://doi.org/10.1016/s0014-3057(02)00173-8
59. Li R, Shan Z (2018) Asynchronous synthesis method of waterborne polyurethane with the differences of structural features and thermal conductivity. J Polym Res 25:197. https://doi.org/10.1007/s10965-018-1577-4
60. Yang Z, Zang H, Wu G (2019) Study of solvent-free sulfonated waterborne polyurethane as an advanced leather finishing material. J Polym Res 26:213. https://doi.org/10.1007/s10965-019-1884-4
61. Song N, Xin X, Liu H, Xu B, Li B, Li Y, Hou S, Yu Y (2019) Effects of different macrodiols as soft segments on properties of waterborne polyurethane. J Polym Res 26:152. https://doi.org/10.1007/s10965-019-1793-6
62. Ren Z, Liu L, Wang H, Fu Y, Jiang L, Ren B (2015) Novel amphoteric polyurethane dispersions with postpolymerization crosslinking function derived from hydroxylated tung oil: synthesis and properties. RSC Adv 5:27717–27721. https://doi.org/10.1039/c5ra03115j
63. Yang X, Ren B, Ren Z, Jiang L, Liu W, Zhu C (2015) Synthesis and properties of novel non-ionic polyurethane dispersion based on Hydroxylated Tung oil and alicyclic Isocyanates. Journal of Materials Science and Chemical Engineering 03:88–94. https://doi.org/10.4236/msce.2015.31013
64. Meuse CW, Yang XZ, Yang DC, Hsu SL (1992) Spectroscopic analysis of ordering and phase-separation behavior of model polyurethanes in a restricted geometry. Macromolecules 25:925–932. https://doi.org/10.1021/ma00028a064
65. Tao H-J, Meuse CW, Yang X, MacKnight WJ, Hsu SL (1994) A spectroscopic analysis of phase separation behavior of polyurethane in restricted geometry: chain rigidity effects. Macromolecules 27:7146–7151. https://doi.org/10.1021/ma00102a023
66. Jiang L, Wu J, Nedolisa C, Saiani A, Assender HE (2015) Phase separation and crystallization in high hard block content polyurethane thin films. Macromolecules 48:5358–5366. https://doi.org/10.1021/acs.macromol.5b01083
67. Kojio K, Uchiba Y, Yamamoto Y, Motokucho S, Furukawa M (2009) Chain and mirophase-separated structures of ultrathin polyurethane films. J Phys Conf Ser 184:012028. https://doi.org/10.1088/1742-6596/184/1/012028
68. Aoki D, Ajiro H (2017) Design of polyurethane composed of only hard main chain with oligo(ethylene glycol) units as side chain simultaneously achieved high biocompatible and mechanical properties. Macromolecules 50:6529–6538. https://doi.org/10.1021/acs.macromol.7b00629
69. Estes GM, Seymour RW, Cooper SL (1971) Infrared studies of segmented polyurethane elastomers. II Infrared Dichroism Macromolecules 4:452–457. https://doi.org/10.1021/ma60022a018
70. Müller-Riederer G, Bonart R (1977) Orientierungsvorgiinge bei der delmung von polyurethan-elastomeren. Progress in Colloids and Polymer Science 62:99–105. https://doi.org/10.1007/BFb0117099
71. Brunette CM, Hsu SL, Macknight WJ (1982) Hydrogen-bonding properties of hard-segment model compounds in polyurethane block copolymers. Macromolecules 15:71–77. https://doi.org/10.1021/ma00229a014
72. Lee HS, Wang YK, Hsu SL (1987) Spectroscopic analysis of phase-separation behavior of model polyurethanes. Macromolecules 20:2089–2095. https://doi.org/10.1021/ma00175a008
73. Koberstein JT, Russell TP (1986) Simultaneous SAXS-DSC study of multiple endothermic behavior in polyether-based polyurethane block copolymers. Macromolecules 19:714–720. https://doi.org/10.1021/ma00157a039
74. Blundell DJ, Eeckhaut G, Fuller W, Mahendrasingam A, Martin C (2002) Real time SAXS/stress-strain studies of thermoplastic polyurethanes at large strains. Polymer 43:5197–5207. https://doi.org/10.1016/s0032-3861(02)00386-5
75. Garrett JT, Lin JS, Runt J (2002) Influence of preparation conditions on microdomain formation in poly(urethane urea) block copolymers. Macromolecules 35:161–168. https://doi.org/10.1021/ma010915d
76. Blundell DJ, Eeckhaut G, Fuller W, Mahendrasingam A, Martin C (2006) Time-resolved SAXS/stress–strain studies of thermoplastic polyurethanes during mechanical cycling at large strains. J Macromol Sci, Part B 43:125–142. https://doi.org/10.1081/mb-120027754
77. Kojio K, Matsuo K, Motokucho S, Yoshinaga K, Shimodaira Y, Kimura K (2011) Simultaneous small-angle X-ray scattering/wide-angle X-ray diffraction study of the microdomain structure of polyurethane elastomers during mechanical deformation. Polym J 43:692–699. https://doi.org/10.1038/pj.2011.48
78. Nozaki S, Hirai T, Higaki Y, Yoshinaga K, Kojio K, Takahara A (2017) Effect of chain architecture of polyol with secondary hydroxyl group on aggregation structure and mechanical properties of polyurethane elastomer. Polymer 116:423–428. https://doi.org/10.1016/j.polymer.2017.03.031
79. Masunaga H, Ogawa H, Takano T, Sasaki S, Goto S, Tanaka T, Seike T, Takahashi S, Takeshita K, Nariyama N, Ohashi H, Ohata T, Furukawa Y, Matsushita T, Ishizawa Y, Yagi N, Takata M, Kitamura H, Sakurai K, Tashiro K, Takahara A, Amamiya Y, Horie K, Takenaka M, Kanaya T, Jinnai H, Okuda H, Akiba I, Takahashi I, Yamamoto K, Hikosaka M, Sakurai S, Shinohara Y, Okada A, Sugihara Y (2011) Multipurpose soft-material SAXS/WAXS/GISAXS beamline at SPring-8. Polym J 43:471–477. https://doi.org/10.1038/pj.2011.18
80. Sui T, Baimpas N, Dolbnya IP, Prisacariu C, Korsunsky AM (2015) Multiple-length-scale deformation analysis in a

thermoplastic polyurethane. Nat Commun 6:6583. https://doi.org/10.1038/ncomms7583
81. Briber RM, Thomas EL (1983) Investigation of 2 crystal forms in MDI BDO-based polyurethanes. J Macromol Sci-Phys B22:509–528. https://doi.org/10.1080/00222348308224773
82. Blackwell J, Gardner KH (1979) Structure of the hard segments in polyurethane elastomers. Polymer 20:13–17. https://doi.org/10.1016/0032-3861(79)90035-1
83. Vanbogart JWC, Gibson PE, Cooper SL (1983) Structure-property relationships in Polycaprolactone-polyurethanes. J Polym Sci B Polym Phys 21:65–95. https://doi.org/10.1002/pol.1983.180210106
84. Pompe G, Pohlers A, Potschke P, Pionteck J (1998) Influence of processing conditions on the multiphase structure of segmented polyurethane. Polymer 39:5147–5153. https://doi.org/10.1016/s0032-3861(97)10350-0
85. Kojio K, Matsumura S, Nozaki S, Motokucho S, Furukawa M, Yoshinaga K, Takahara A (2014) Crystallization behavior of hard segment in polyurethane elastomers. Kobunshi Ronbunshu 71:608–614. https://doi.org/10.1295/koron.71.608
86. McLean RS, Sauer BB (1997) Tapping-mode AFM studies using phase detection for resolution of nanophases in segmented polyurethanes and other block copolymers. Macromolecules 30:8314–8317. https://doi.org/10.1021/ma970350e
87. Kojio K, Kugumiya S, Uchiba Y, Nishino Y, Furukawa M (2009) The microphase-separated structure of polyurethane bulk and thin films. Polym J 41:118–124. https://doi.org/10.1295/polymj.PJ2008186
88. Garrett JT, Siedlecki CA, Runt J (2001) Microdomain morphology of poly(urethane urea) multiblock copolymers. Macromolecules 34:7066–7070. https://doi.org/10.1021/ma0102114
89. Akram N, Zia KM, Saeed M, Mansha A, Khan WG (2018) Morphological studies of polyurethane based pressure sensitive adhesives by tapping mode atomic force microscopy. J Polym Res 25:194. https://doi.org/10.1007/s10965-018-1591-6
90. Petrovic ZS, Budinski-Simendic J (1985) Study of the effect of soft segment length and concentration on properties of polyetherurethanes. I. the effect on physical and morphological properties. Rubber Chem Technol 58:685–700
91. Petrovic ZS, Budinski-Simendic J (1985) Study of the effect of soft segment length and concentration on properties of polyetherurethanes. I. the effect on physical and morphological properties. Rubber Chem Technol 58:701–712
92. Sheth JP, Klinedinst DB, Wilkes GL, Yilgor I, Yilgor E (2005) Role of chain symmetry and hydrogen bonding in segmented copolymers with monodisperse hard segments. Polymer 46:7317–7322. https://doi.org/10.1016/j.polymer.2005.04.041
93. Sami S, Yildirim E, Yurtsever M, Yurtsever E, Yilgor E, Yilgor I, Wilkes GL (2014) Understanding the influence of hydrogen bonding and diisocyanate symmetry on the morphology and properties of segmented polyurethanes and polyureas: computational and experimental study. Polymer 55:4563–4576. https://doi.org/10.1016/j.polymer.2014.07.028
94. Xie R, Bhattacharjee D, Argyropoulos J (2009) Polyurethane elastomers based on 1,3 and 1,4-bis(isocyanatomethyl)cyclohexane. J Appl Polym Sci 113:839–848. https://doi.org/10.1002/app.29934
95. Kojio K, Rahmawati R, Shinohara N, Yamasaki S (2019) Molecular aggregation structure and mechanical properties of low-hard segment content polyurethane and polythiourethane elastomers based on cycloaliphatic diisocyanate with a symmetric structure. J Adhes Soc Jpn 55:181–185
96. Petrovic ZS, Ilavsky M, Dusek K, Vidakovic M, Javni I, Banjanin B (1991) The effect of cross-linking on properties of polyurethane elastomers. J Appl Polym Sci 42:391–398. https://doi.org/10.1002/app.1991.070420211
97. Petrovic ZS, Javni I, Banhegy G (1998) Mechanical and dielectric properties of segmented polyurethane elastomers containing chemical crosslinks in the hard segment. J Polym Sci B Polym Phys 36:237–251. https://doi.org/10.1002/(sici)1099-0488(19980130)36:2<237::aid-polb4>3.0.co;2-o
98. Furukawa M, Hamada Y, Kojio K (2003) Aggregation structure and mechanical properties of functionally graded polyurethane elastomers. J Polym Sci B Polym Phys 41:2355–2364. https://doi.org/10.1002/polb.10628
99. Kojio K, Matsumura S, Komatsu T, Nozaki S, Motokucho S, Furukawa M, Yoshinaga K (2014) Microphase-separated structure and dynamic viscoelastic properties of polyurethanes elastomers prepared at various temperatures and cross-linking agent contents. Nihon Reoroji Gakkaishi 42:143–149. https://doi.org/10.1678/rheology.42.143
100. Kojio K, Nakamura S, Furukawa M (2008) Effect of side groups of polymer glycol on microphase-separated structure and mechanical properties of polyurethane elastomers. J Polym Sci B Polym Phys 46:2054–2063. https://doi.org/10.1002/polb.21540
101. Camberlin Y, Pascault JP, Letoffe JM, Claudy P (1982) Synthesis and DSC study of model hard segments from Diphenyl methane Diisocyanate and butane Diol. J Polym Sci, Part A: Polym Chem 20:383–392. https://doi.org/10.1002/pol.1982.170200212
102. Hwang KKS, Wu GS, Lin SB, Cooper SL (1984) Synthesis and characterization of MDI-butanediol urethane model compounds. J Polym Sci, Part A: Polym Chem 22:1677–1697. https://doi.org/10.1002/pol.1984.170220714
103. Li Q, Zhou H, Wicks DA, Hoyle CE, Magers DH, McAlexander HR (2009) Comparison of small molecule and polymeric urethanes, thiourethanes, and dithiourethanes: hydrogen bonding and thermal, physical, and mechanical properties. Macromolecules 42:1824–1833. https://doi.org/10.1021/ma802848t
104. Shin J, Matsushima H, Chan JW, Hoyle CE (2009) Segmented polythiourethane elastomers through sequential thiol− ene and thiol− isocyanate reactions. Macromolecules 42:3294–3301. https://doi.org/10.1021/ma8026386
105. Laity PR, Taylor JE, Wong SS, Khunkamchoo P, Norris K, Cable M, Chohan V, Andrews GT, Johnson AF, Cameron RE (2006) Mechanical deformation of polyurethanes. J Macromol Sci, Part B 43:95–124. https://doi.org/10.1081/mb-120027753
106. Shibayama M, Kawauchi T, Kotani T, Nomura S, Matsuda T (1986) Structure and properties of fatigued segmented Poly(urethaneurea) I. Segment orientation mechanism due to fatigue. Polym J 18:719–733. https://doi.org/10.1295/polymj.18.719
107. Shibayama M, Ohki Y, Kotani T, Nomura S (1987) Structure and properties of fatigued segmented poly(urethaneurea)s II. Structural analyses of fatigue mechanism. Polym J 19:1067–1080. https://doi.org/10.1295/polymj.19.1067
108. Unsal E, Yalcin B, Yilgor I, Yilgor E, Cakmak M (2009) Real time mechano-optical study on deformation behavior of PTMO/CHDI-based polyetherurethanes under uniaxial extension. Polymer 50:4644–4655. https://doi.org/10.1016/j.polymer.2009.07.041